

Supplementary Information

A rapid “on-off-on” mitochondria-targeted phosphorescent probe for  
selective and consecutive detection of Cu<sup>2+</sup> and Cysteine in live cells and  
zebrafish

**Peipei Deng<sup>†a</sup>, Yongyan Pei<sup>†a</sup>, Mengling Liu<sup>a</sup>, Wenzhu Song<sup>a</sup>, Mengru Wang<sup>a</sup>,**

**Feng Wang<sup>b,\*</sup>, Chunxian Wu<sup>a</sup>, Li Xu<sup>a,\*</sup>**

*<sup>a</sup>School of Chemistry and Chemical Engineering, Guangdong Pharmaceutical  
University, Zhongshan, 528458, P. R. China*

*<sup>b</sup>School of Food and Biological Engineering, Hefei University of Technology, Hefei,  
230009, P. R. China*

E-mail: [xuli473@163.com](mailto:xuli473@163.com)(L. Xu), [fengw420@hfut.edu.cn](mailto:fengw420@hfut.edu.cn) (F. Wang)

<sup>†</sup> These authors contributed equally to this work.

## Experimental Procedures

### Detection limit

The detection limit was obtained with the phosphorescence titration. The standard deviation of the blank measurement was determined based on six times of the phosphorescence intensities of **Ir** or **Ir-Cu** ensemble. The detection limit was calculated by the  $3\sigma/k$  equation, where  $\sigma$  represented the standard deviation of blank measurement,  $k$  denoted the slope between the phosphorescence intensity versus the concentrations of analytes.<sup>1</sup>

### <sup>1</sup>H NMR experiment

Three NMR tubes of **Ir** (5 mg, 5  $\mu$ mol) were prepared by dissolving in DMSO-*d*6 (400  $\mu$ L), and then 0, 0.5, and 1 equiv. of Cu<sup>2+</sup> dissolved in D<sub>2</sub>O (100  $\mu$ L) were added to **Ir**, respectively. Sequentially, 1 equiv. of Cu<sup>2+</sup> dissolved in D<sub>2</sub>O (100  $\mu$ L) was added to one NMR tube of **Ir** (5 mg, 5  $\mu$ mol) dissolved in DMSO-*d*6 (300  $\mu$ L), and then 2 equiv. of Cys dissolved in D<sub>2</sub>O (100  $\mu$ L) was added to the mixture. <sup>1</sup>H NMR spectra were obtained at room temperature after shaking them for minutes.

### Cell imaging experiments

In the cellular co-localization experiment, adherent HeLa cells in confocal dishes at a density of  $1 \times 10^4$  cells/mL were exposed to **Ir** (5  $\mu$ M) at 37 °C for 1 h. After that, the cells were washed with PBS and further stained by 50 nM Mito-Tracker Red for 30 min. The cells were washed three times with PBS and the phosphorescence signals were acquired on a Zeiss LSM 710 NLO confocal microscope (63 $\times$ /NA 1.4 oil immersion objective).

For reversible imaging of Cu<sup>2+</sup> ions and Cys, culture dishes with *ca.*  $1 \times 10^4$  HeLa cells were incubated with **Ir** (5  $\mu$ M) for 1 h, and the cells were washed with PBS for three times. The **Ir**-loaded cells were sequentially incubated with Cu<sup>2+</sup> (5  $\mu$ M, 0.5 h) and Cys (10  $\mu$ M, 0.5 h), respectively. Upon completion, the cells were washed with PBS solution for three times to remove remaining compounds and ions, prior to the observation by confocal microscopy.

For the detection of endogenous Cys, culture dishes with *ca.*  $1 \times 10^4$  HeLa cells were incubated with **Ir-Cu** ensemble (5  $\mu$ M, 1 h) at 37 °C. The cells were washed three times with PBS before subjected to a confocal microscopy. To detect exogenous reactive thiols, four culture dishes with *ca.*  $1 \times 10^4$  HeLa cells were pretreated with NEM (0.5 mM, 0.5 h), and incubated with **Ir-Cu** ensemble (5  $\mu$ M, 1 h) and further treated without or with Cys, Hcy or GSH (0.1 mM, 0.5 h), respectively. After three rinses in PBS, the cells imaging was obtained on a confocal laser scanning microscope.

### **Cytotoxicity assay**

The cytotoxic effect of **Ir** was studied by the MTT assay with HeLa cell lines.<sup>2</sup> First, 96-well plates were seeded with HeLa cells (approximately  $1 \times 10^4$  cells per well) and cultured for 24 h. Then various concentrations of the tested complex was added to the cells and incubated for 12 h. Upon completion, HeLa cells were washed with PBS, and changed into 20  $\mu$ L, 5 mg·mL<sup>-1</sup> MTT stock dye solution and further incubated for 4 h. The medium containing MTT was removed carefully and 150  $\mu$ L of dimethyl sulfoxide was added to each well. The plate was analyzed on a microplate

spectrophotometer at a wavelength of 540 nm to measure the optical density (OD). Three independent experiments were performed and expressed as mean  $\pm$  standard deviation.

### **ICP-MS analysis**

Three culture dishes with *ca.*  $1 \times 10^5$  HeLa cells were incubated with 5  $\mu\text{M}$  **Ir** for 6 h at 37 °C. After digestion, HeLa cells were accurately counted, divided into equal portions. The nucleus, cytoplasm and mitochondria were isolated using nucleus extraction kit, cytoplasm extraction kit and mitochondria extraction kit respectively (Pierce, Thermo). The acquired samples were digested by 60% nitric acid at room temperature overnight, and then diluted with dd water to 10 mL with 3% of nitric solutions.<sup>3</sup> The iridium(III) concentration in the three portions was determined by inductively coupled plasma mass spectrometry (ICP-MS Thermo Elemental Co., Ltd.). Data were reported as the mean  $\pm$  standard deviation ( $n = 3$ ).

### **Flow cytometry analysis**

HeLa cells were seeded at a density of  $1 \times 10^5$  cells per mL in 6-well plates for 24 h in an incubator. To analyze the reversible phosphorescence response of **Ir** towards  $\text{Cu}^{2+}$  ions and Cys, cells were treated with **Ir** (5  $\mu\text{M}$ ) for 1 h. After that,  $\text{Cu}^{2+}$  ions (5  $\mu\text{M}$ ) was supplemented for 30 min, following by adding Cys (10  $\mu\text{M}$ ) for another 30 min. To assess the phosphorescence response on different concentrations of  $\text{Cu}^{2+}$  and Cys by **Ir**, 6-well plates with *ca.*  $1 \times 10^5$  HeLa cells were treated with **Ir** (5  $\mu\text{M}$ , 1 h), then incubated with  $\text{Cu}^{2+}$  ions at various concentrations for 0.5 h, finally incubated various concentrations of Cys solutions for 0.5 h.

For the analysis of endogenous Cys, HeLa cells were incubated with **Ir-Cu** ensemble (5  $\mu$ M, 1 h) at 37 °C, and then the media was replaced with PBS buffer. Cells were also pre-treated with NEM (0, 50, 100, and 500  $\mu$ M) for 0.5 h, and then with **Ir-Cu** ensemble (5  $\mu$ M) for another 1 h. For the analysis of exogenous Cys, HeLa cells treated with NEM for 0.5 h were incubated with **Ir-Cu** ensemble (5  $\mu$ M, 1 h), and then further incubated with 0.1 mM Cys, GSH or Hcy for another 0.5 h, respectively. 0.05% trypsin-EDTA solution detached all the cells from the well. These cell samples were washed three times with PBS and analyzed on a FACS Canto II instrument (BD Biosciences, USA). At least 10000 cells were counted at each experiment. Cells treated with culture medium for 24 h were regarded as the controls for all experiments.

### **Imaging of zebrafish**

Healthy male and female zebrafish were incubated in different tanks with a 12 h light/12 h dark cycle at 28 °C, and then the spawning of eggs was obtained by giving light stimulation in the morning. Almost all the eggs were fertilized immediately and cultured in E3 embryo media (15 mM NaCl, 0.5 mM KCl, 1 mM MgSO<sub>4</sub>, 1 mM CaCl<sub>2</sub>, 0.15 mM KH<sub>2</sub>PO<sub>4</sub>, 0.05 mM Na<sub>2</sub>HPO<sub>4</sub>, 0.7 mM NaHCO<sub>3</sub>, 10<sup>-5</sup> % methylene blue; pH 7.5) at 28 °C.

Zebrafish (5 days old) were incubated with or without NEM (0.5 mM) for 0.5 h, and further incubated with **Ir-Cu** ensemble (5  $\mu$ M) for another 30 min. **Ir-Cu** ensemble incubated zebrafish were further treated with Cys, GSH, Hcy (0.1 mM) at 28 °C for 30 min, respectively. The zebrafish was washed with E3 media for three

times before subjected to a fluorescence inversion microscopy (Olympus U-HGLGPS). Untreated zebrafish were used as black controls.

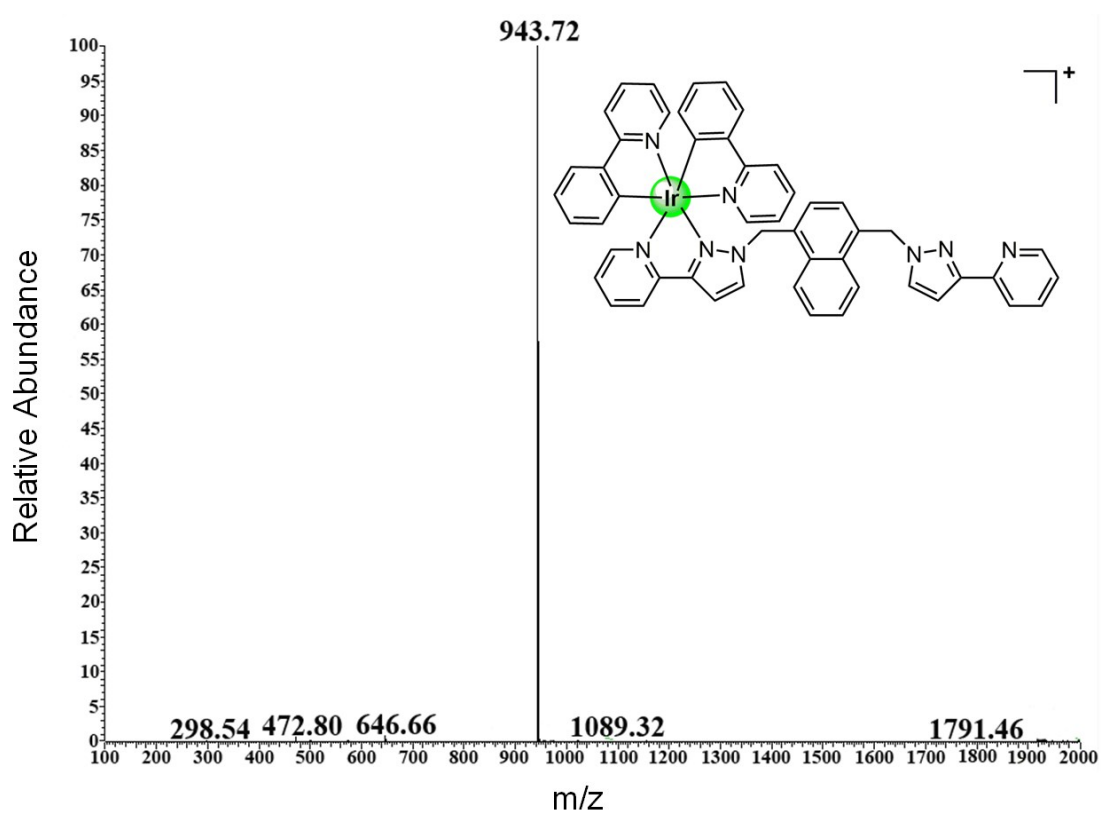


Figure S1. ESI-MS spectrum of **Ir**.

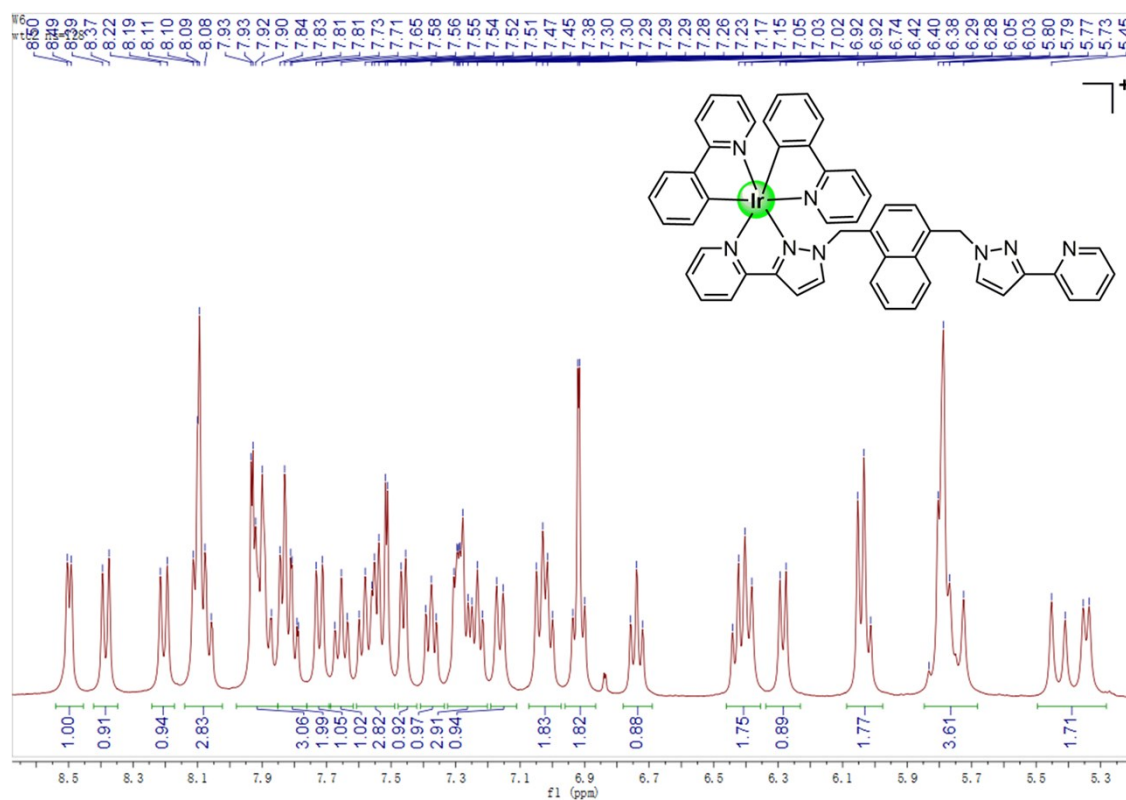


Figure S2. <sup>1</sup>H NMR spectrum (400 MHz) of Ir in DMSO-d<sub>6</sub>.

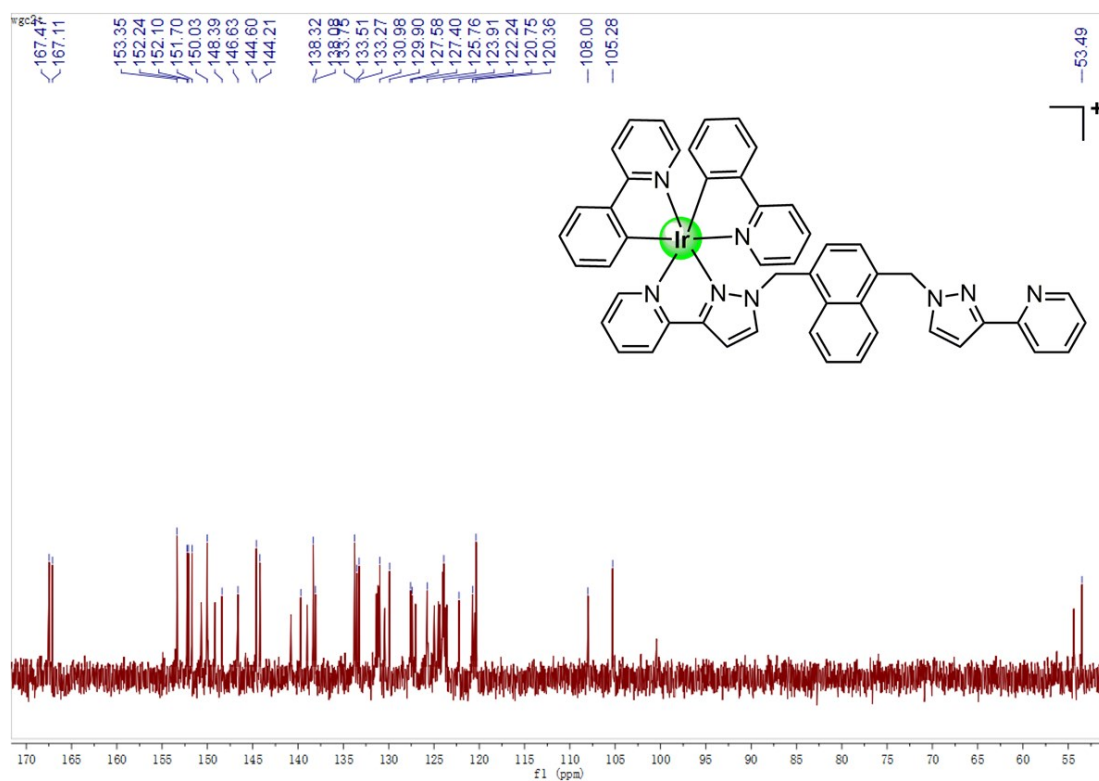


Figure S3. <sup>13</sup>C NMR spectrum (101 MHz) of Ir in DMSO-d<sub>6</sub>.

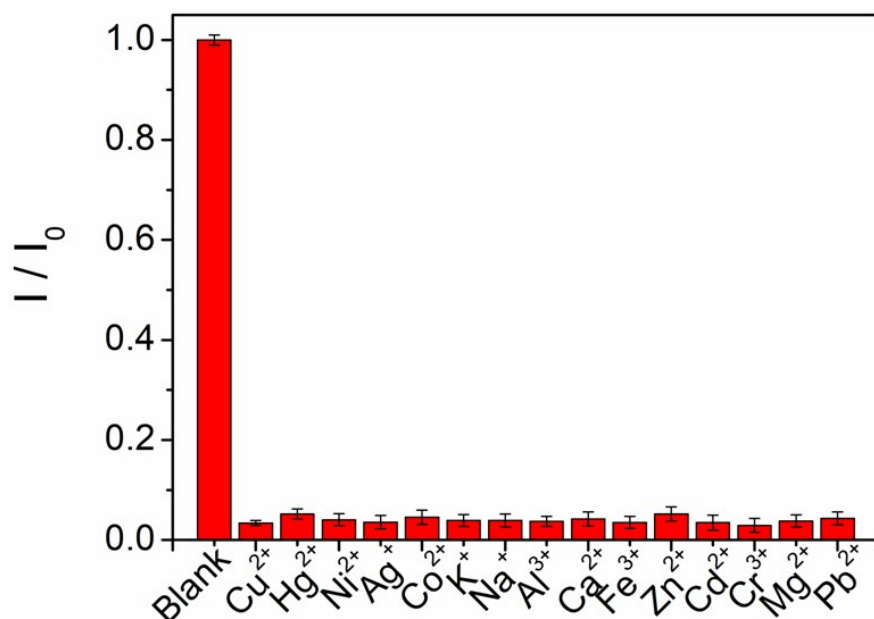


Figure S4. The phosphorescence intensity of **Ir** (5  $\mu\text{M}$ ) upon the addition of  $\text{Cu}^{2+}$  (5  $\mu\text{M}$ ) in the presence of background metal ions (20  $\mu\text{M}$ ) in HEPES buffer solution (pH 7.4);  $\lambda_{\text{ex}} = 376 \text{ nm}$ ,  $\lambda_{\text{em}} = 486 \text{ nm}$ .

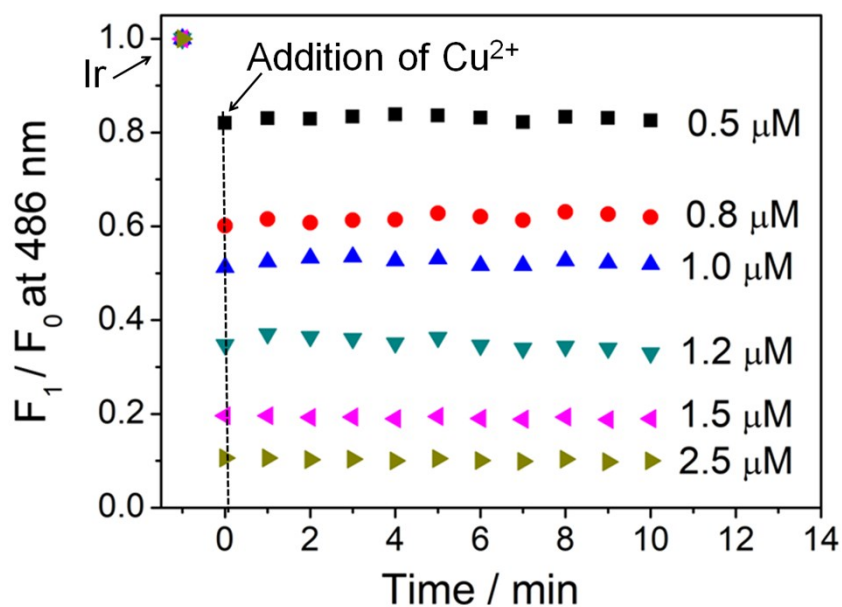


Figure S5 Effect of incubation time on phosphorescence intensity at 486 nm of **Ir** (5  $\mu\text{M}$ ) following the addition of different concentrations of  $\text{Cu}^{2+}$  (0.5 - 2.5  $\mu\text{M}$ ) in HEPES buffer (10 mM, pH 7.4),  $\lambda_{\text{ex}} = 376 \text{ nm}$ .



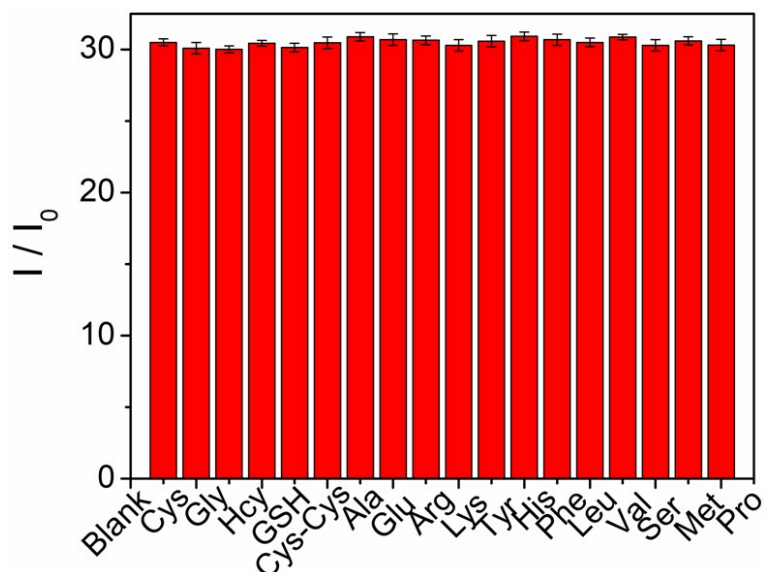


Figure S6. Phosphorescence response of the **Ir-Cu** ensemble ( $[\text{Ir}] = 5 \mu\text{M}$ ,  $[\text{Cu}^{2+}] = 5 \mu\text{M}$ ) at 486 nm toward Cys ( $10 \mu\text{M}$ ) in the presence of different interferes ( $30 \mu\text{M}$ );  $\lambda_{\text{ex}} = 376 \text{ nm}$ .

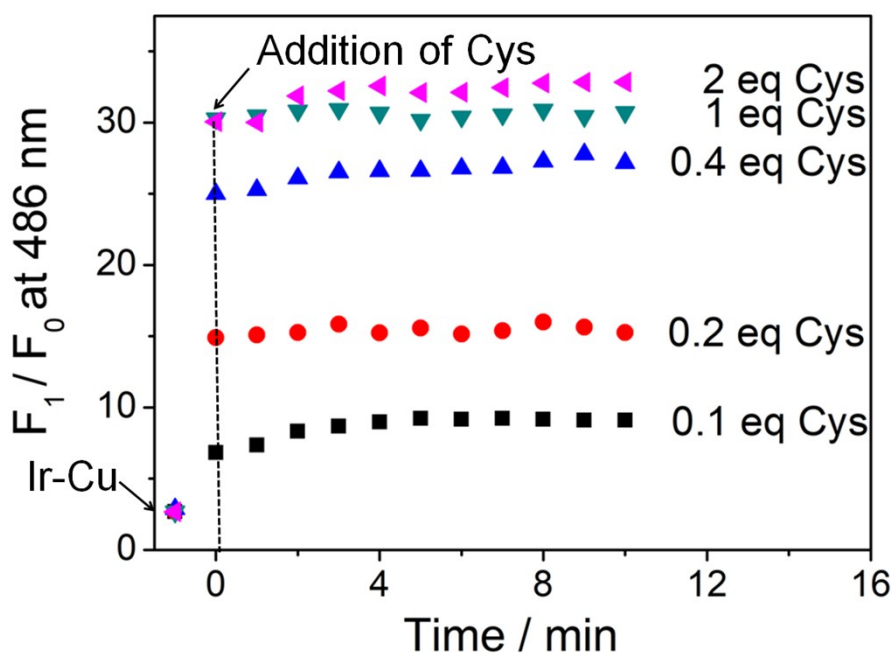


Figure S7 Effect of incubation time on phosphorescence intensity at 486 nm of the **Ir-Cu** ensemble ( $5 \mu\text{M}$ ) in HEPES buffer ( $10 \text{ mM}$ ,  $\text{pH } 7.4$ ) in the presence of Cys with different concentrations from 0.1 eq to 2 eq.  $\lambda_{\text{ex}} = 376 \text{ nm}$ .

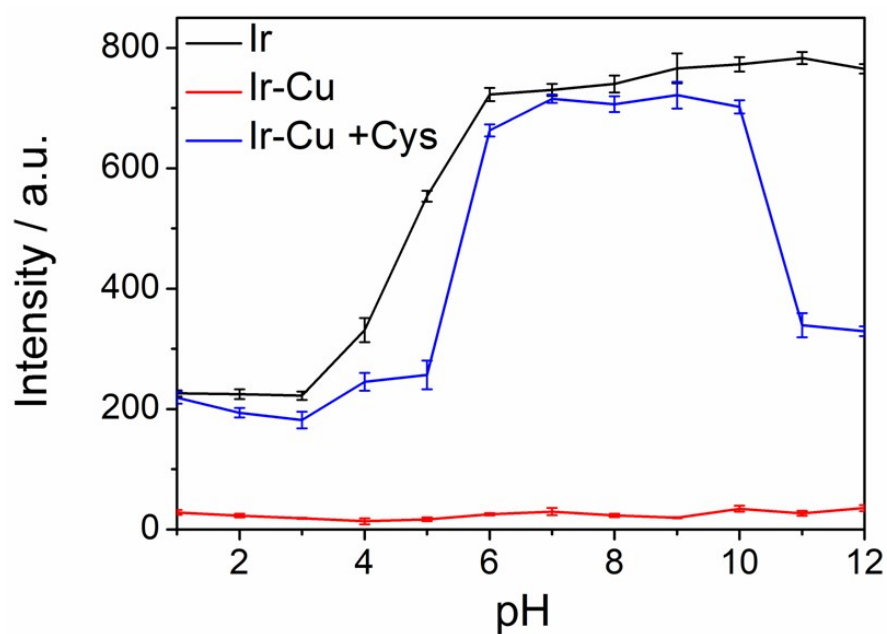


Figure S8 pH-dependent phosphorescence intensities of **Ir** (5 μM), **Ir-Cu** ensemble (5 μM) in the absence and presence of Cys (10 μM) in HEPES buffer (10 mM, pH 7.4).

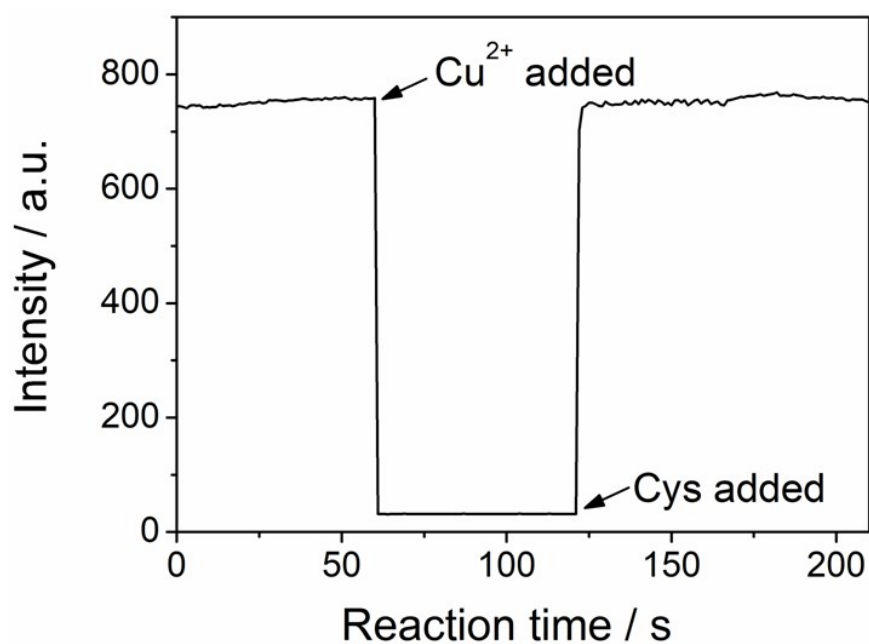


Figure S9 Real-time phosphorescence responses of **Ir** (5 μM) upon addition of Cu<sup>2+</sup> (5 μM) followed by Cys (10 μM).

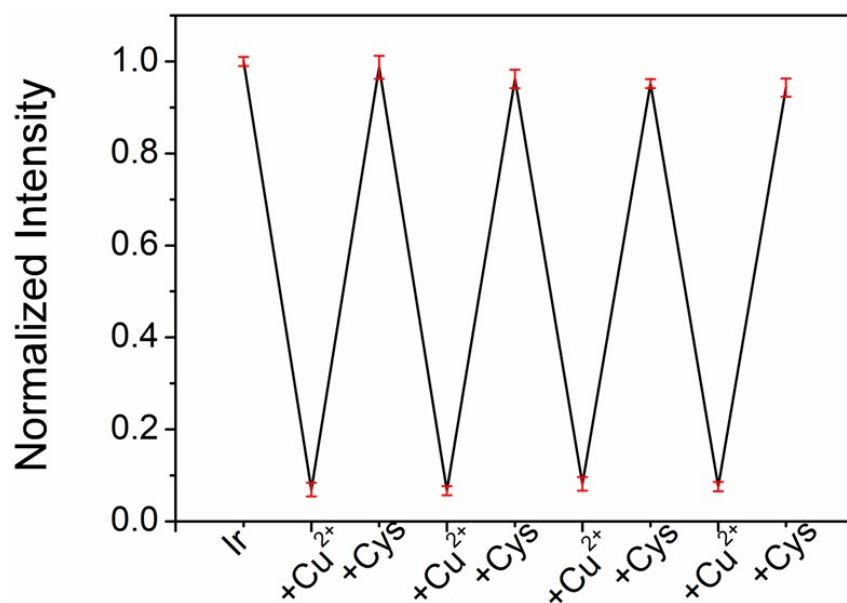


Figure S10 Phosphorescence intensity of **Ir** (5  $\mu$ M) at 486 nm upon the alternative addition of  $\text{Cu}^{2+}$  (5  $\mu$ M) and Cys (10  $\mu$ M) in HEPES buffer (10 mM, pH 7.4).

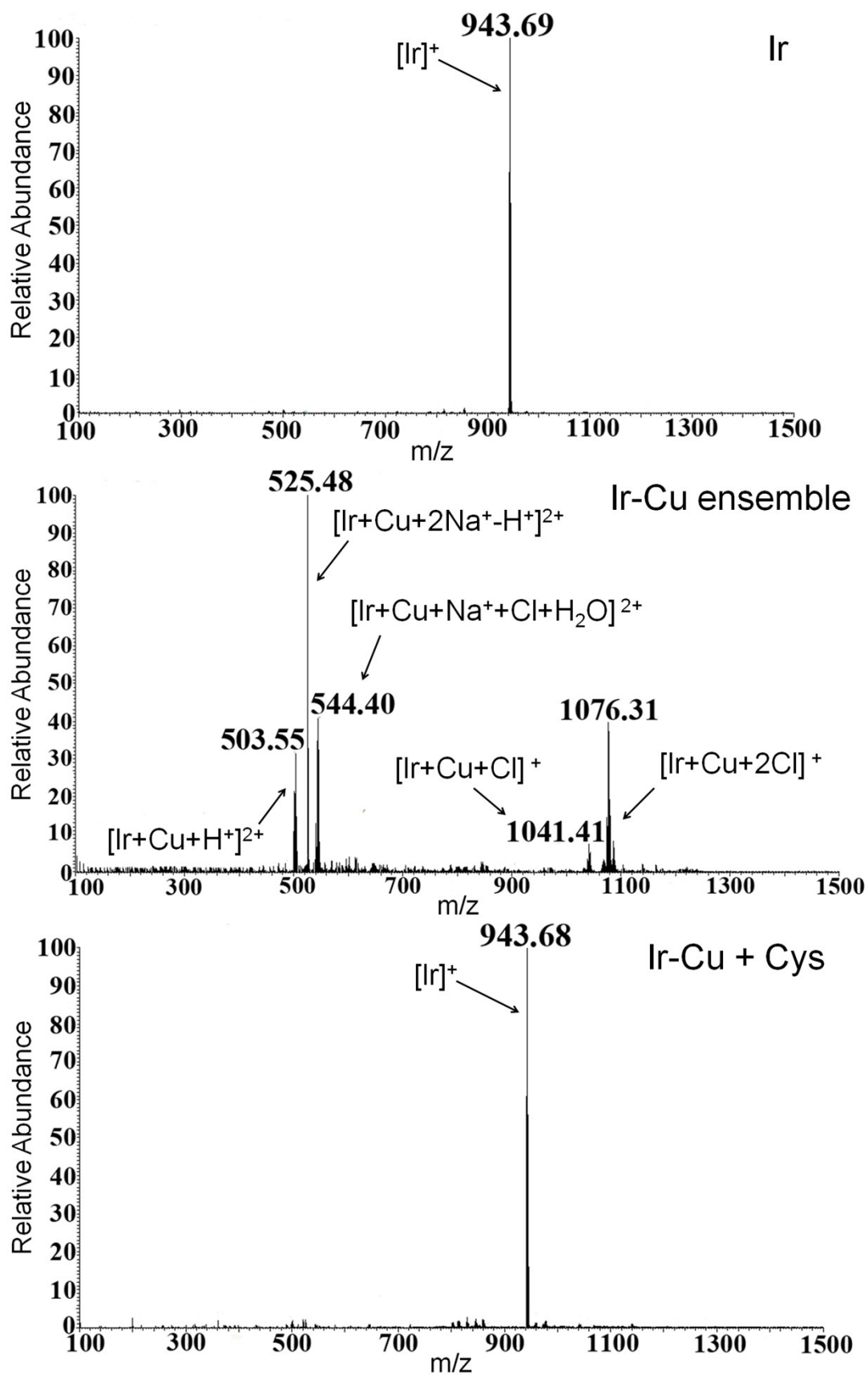


Figure S11 The ESI-MS spectra of **Ir** and the **Ir-Cu** ensemble without or with Cys.

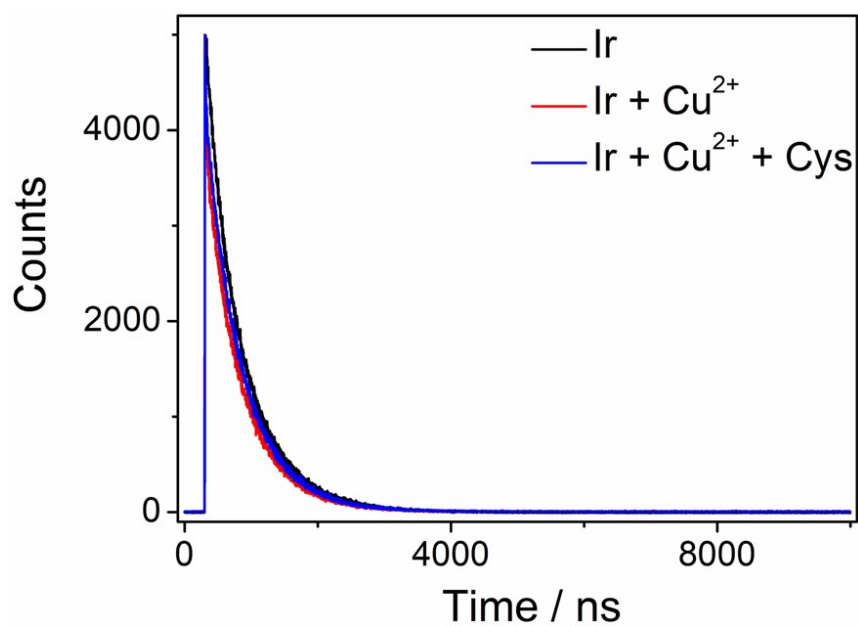


Figure S12 Phosphorescence decay curve for **Ir** after the addition of Cu<sup>2+</sup> and Cys.

The measurement is made at  $\lambda_{\text{em}} = 486 \text{ nm}$ .

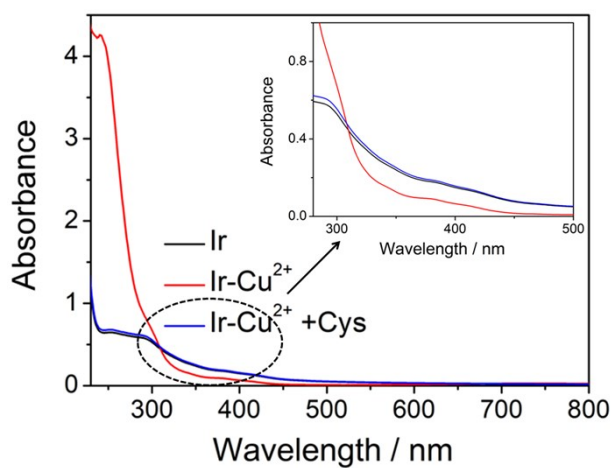


Figure S13 UV-vis absorption spectra of **Ir** (5  $\mu\text{M}$ ), **Ir** (5  $\mu\text{M}$ ) + Cu<sup>2+</sup> (5  $\mu\text{M}$ ) system and **Ir** (5  $\mu\text{M}$ ) + Cu<sup>2+</sup> (5  $\mu\text{M}$ ) + Cys (10  $\mu\text{M}$ ) system.

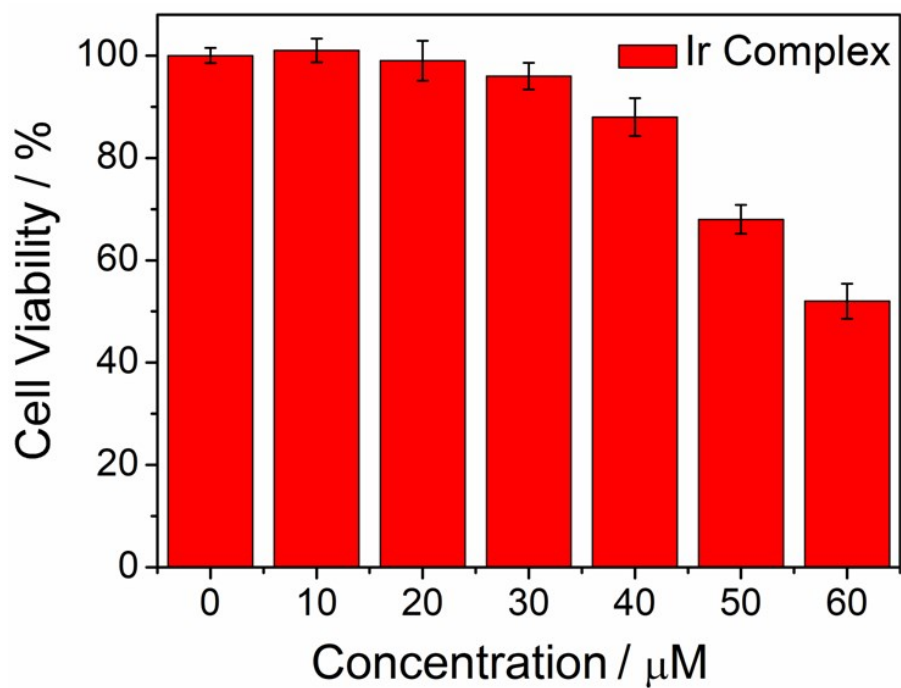


Figure S14 *In vitro* cell viability of HeLa cells incubated with **Ir** (0-60  $\mu\text{M}$ ) at 37 °C for 24 h.

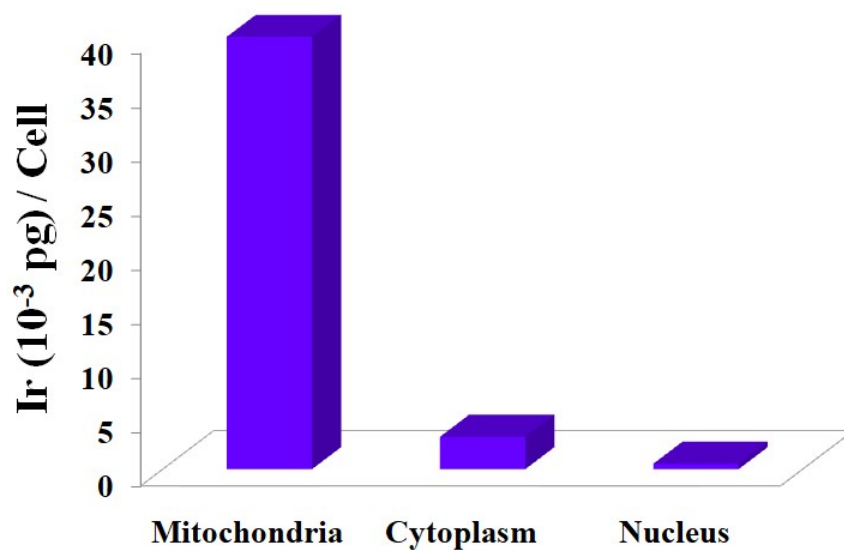


Figure S15 Distribution analysis of **Ir** in HeLa cells by ICP-MS.

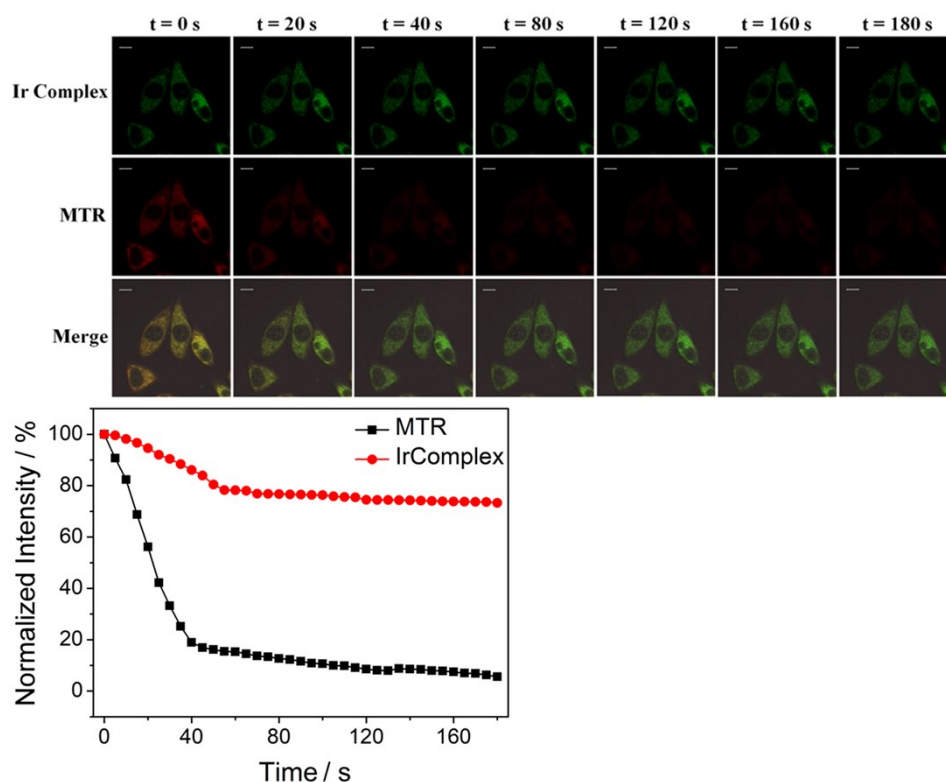


Figure S16 The anti-bleaching properties of **Ir**. HeLa cells were treated with **Ir** (5  $\mu$ M), followed by MTR (50 nM). (a) Confocal images of cells stained with **Ir** and MTR with an increasing bleaching time (180 s). (b) Intensity loss (%) of the phosphorescence of **Ir** and MTR with an increasing bleaching time.

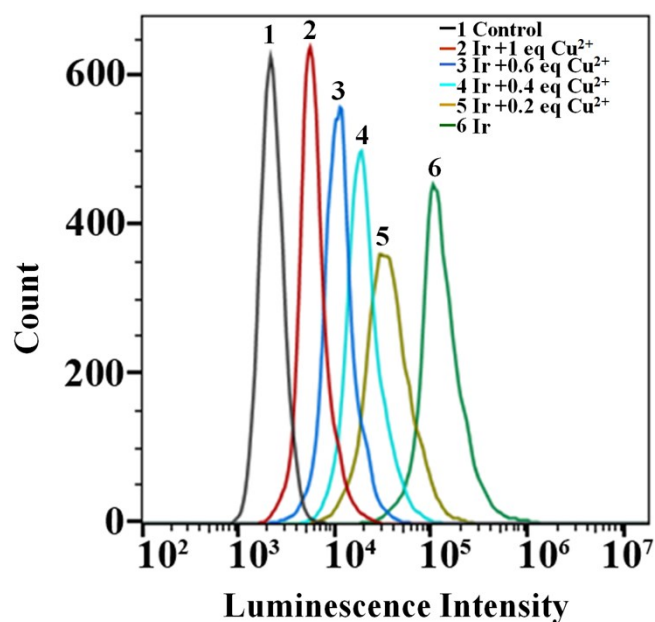


Figure S17 Flow cytometry analysis of HeLa cells after incubation with **Ir** (5  $\mu$ M) for

1 h in the absence and the presence of 0.2 eq, 0.4 eq, 0.6 eq, and 1 eq  $\text{Cu}^{2+}$ . Control group, HeLa cells only.

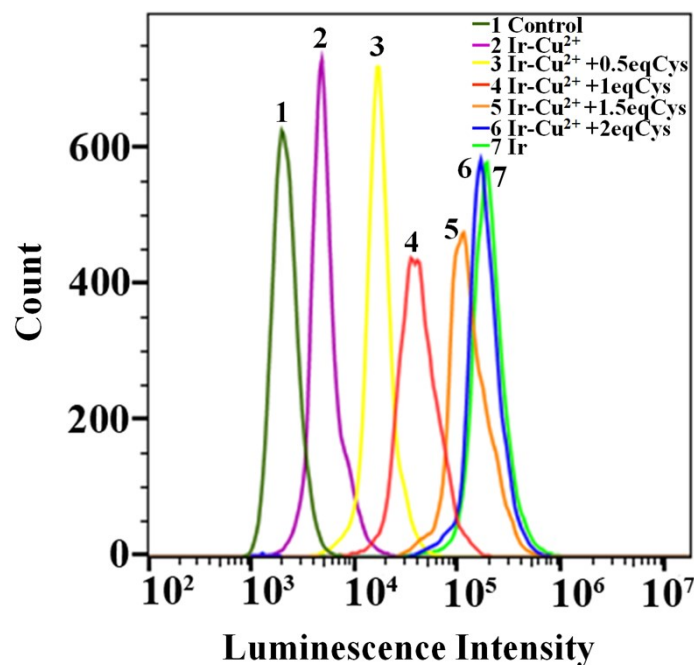


Figure S18 Representative flow cytometry histograms of HeLa cells loaded with **Ir**, **Ir-Cu** ensemble and **Ir-Cu** ensemble in the presence of 0.5 eq, 1 eq, 1.5 eq, and 2 eq Cys. Control group, HeLa cells only.

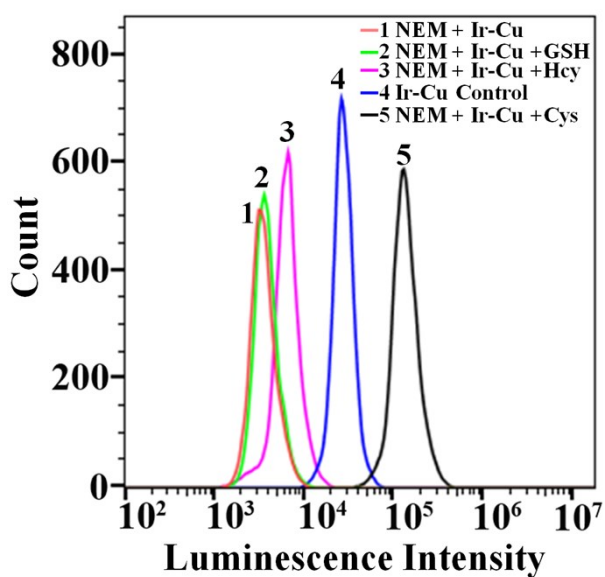


Figure S19. Flow cytometry analysis of HeLa cells after incubation with the **Ir-Cu**



ensemble (5  $\mu\text{M}$ ) for 1 h or HeLa cells preincubated with NEM (0.5 mM) for 30 min, and then treated with Cys (0.1 mM), Hcy (0.1 mM) or GSH (0.1 mM) for 30 min, respectively, followed by the **Ir-Cu** ensemble (5  $\mu\text{M}$ ) for 1 h.

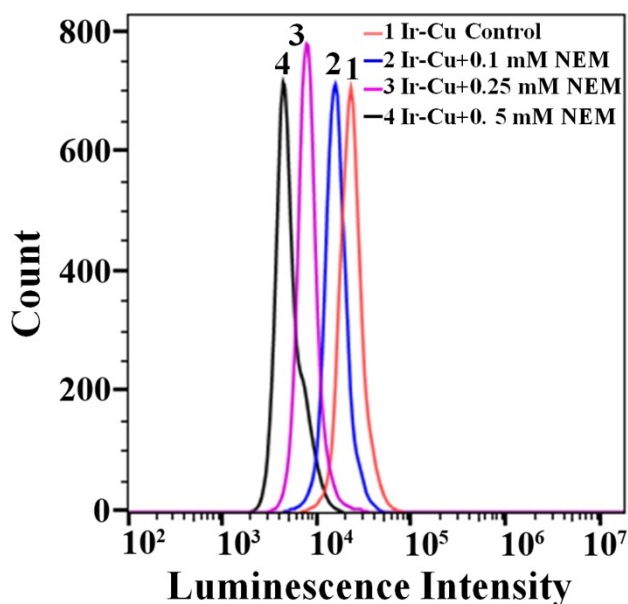


Figure S20. Flow cytometry analysis of HeLa cells after incubation with the **Ir-Cu** ensemble (5  $\mu\text{M}$ ) for 1 h without and with NEM (0.1 mM, 0.25 mM, and 0.5 mM).

Table S1 Comparison table of **Ir-Cu** ensemble with some reported fluorescent sensor for Cys.

Probes	Water fraction	Analyte	Detection limit ( $\mu\text{M}$ )	Applications	Ref
FSD-103-Cu <sup>2+</sup>	90%	Cys	0.2		4
NRQDs-Cu <sup>2+</sup>	100%	Cys	0.03	Live cell imaging	5
Cu-1	99%	Cys	0.084	Live cell imaging	6
PTCO2-Cu(II)	100%	Cys	0.33	Live cell imaging	7
PQD-Cu <sup>2+</sup>	100%	Cys	28.11	Logic Gate Operation	8

PEIN-Cu <sup>2+</sup>	100%	Cys, GSH	2.7, 7.4	molecular logic gate	9
L-Cu <sup>2+</sup>	30%	Cys, Hcy, GSH	0.96, 0.68, 0.44	Real sample analysis	10
Ru-DPA-Cu	100%	Cys, His	0.24, 1.38	Live cell and zebrafish imaging	11
Si-CDs@ Cu <sup>2+</sup>	100%	Cys	0.41	Live cell imaging	12
Ir-Cu	99%	Cys	0.054	Live cell and zebrafish imaging	This work

## References

- [1] L. Xu, W. H. Zhou, J. W. Liu, Enhanced DNA sensitized Tb<sup>3+</sup> luminescence in organic solvents for more sensitive detection, *Anal. Chim. Acta.*, 2017, **977**, 44-51.
- [2] Y. C. Wang, C. Qian, Z. L. Peng, X. J. Hou, L. L. Wang, H. Chao, L. N. Ji, Dual topoisomerase I and II poisoning by chiral Ru(II) complexes containing 2-thiophenylimidazo[4,5-f][1,10]phenanthroline derivatives, *J. Inorg. Biochem.*, 2014, **130**, 15-27.
- [3] A. E. Egger, C. Rappel, M. A. Jakupiec, C. G. Hartinger, P. Heffeter, B. K. Keppler, Development of an experimental protocol for uptake studies of metal compounds in adherent tumor cells, *J. Anal. Spectrom.*, 2009, **24**, 51-61.
- [4] Y. Cai, J. K. Fang, H. S. Zhu, W. W. Qin, Y. R. Cao, H. J. Yu, G. Shao, Y. J. Liu, W. P. Liu, A rapid “off-on” copper-induced AIE active sensor for fluorimetric detection of cysteine, *Sens. Actuators B-Chem.*, 2020, **303**, 127214.
- [5] T. T. Gu, W. Zou, F. C. Gong, J. Y. Xia, C. Chen, X. J. Chen, A specific nanoprobe for cysteine based on nitrogen-rich fluorescent quantum dots combined with Cu<sup>2+</sup>, *Biosens. Bioelectron.*, 2018, **100**, 79-84.

- [6] H. Fang, N. Wang, L. Xie, P. Huang, K. Deng and F. Wu, An excited-state intramolecular proton transfer (ESIPT)-based aggregation-induced emission active probe and its Cu(II) complex for fluorescence detection of cysteine, *Sens. Actuators B-Chem.*, 2019, **294**, 69-77.
- [7] L. H. Liu, Q. Zhang, J. Wang, L. L. Zhao, L. X. Liu, Y. Lu, A specific fluorescent probe for fast detection and cellular imaging of cysteine based on a water-soluble conjugated polymer combined with copper(II), *Talanta*, 2019, **198**, 128-136.
- [8] X. R. Liu, S. X. Zhang, H. Xu, R. R. Wang, L. N. Dong, S. M. Gao, B. Y. Tang, W. N. Fang, F. J. Hou, L. L. Zhong, A. Aldalbahi, Nitrogen-doped carbon quantum dots from poly(ethyleneimine) for optical dual-mode determination of Cu<sup>2+</sup> and L-Cysteine and Their Logic Gate Operation, *ACS Appl. Mater. Interfaces*, 2020, **12**, 47245-47255.
- [9] X. N. Qin, Q. Tong, M. Y. Chang, S. C. Liang, A hydrophilic polymer-based bifunctional nanosensor for sequential fluorescence sensing of Cu<sup>2+</sup> and biothiols and constructing molecular logic gate, *J. Photochem. Photobiol A: Chemistry*, 2020, **402**, 112792.
- [10] Y. Wang, H. Feng, H. B. Li, X. Y. Yang, H. M. Jia, W. J. Kang, Q. T. Meng, Z. Q. Zhang, R. Zhang, A copper (II) ensemble-based fluorescence chemosensor and its application in the ‘naked-eye’ detection of biothiols in human urine, *Sensors*, 2020, **20**, 1331.
- [11] Y. T. Yang, Y. B. Li, X. M. Zhi, Y. J. Xu, M. N. Li, A red-emitting luminescent probe for sequentially detecting Cu<sup>2+</sup> and cysteine/histidine in aqueous solution and

its imaging application in living zebrafish, *Dyes Pigments*, 2020, **183**, 108690.

- [12] M. H. Zan, C. Li, D. M. Zhu, L. Rao, Q. F. Meng, B. Chen, W. Xie, X. W. Qie, L. Li, X. J. Zeng, Y. R. Li, W. F. Dong, W. Liu, A novel “on–off–on” fluorescence assay for the discriminative detection of Cu(II) and l-cysteine based on red-emissive Si-CDs and cellular imaging applications, *J. Mater. Chem. B*, 2020, **8**, 919-927.